

*Supporting information*

# Synthesis, Characterization, Photoluminescence, Molecular Docking and Bioactivity of Zinc (II) Compounds Based on Different Substituents

Rongping Liu <sup>1,2</sup>, Hao Yan <sup>3</sup>, Jinzhang Jiang <sup>1</sup>, Jiahe Li <sup>1</sup>, Xing Liang <sup>1</sup>, Dengfeng Yang <sup>4</sup>, Lixia Pan <sup>2,\*</sup>, Tisan Xie <sup>3,\*</sup> and Zhen Ma <sup>1,\*</sup>

<sup>1</sup> School of Chemistry and Chemical Engineering, Guangxi University, Nanning 530004, Guangxi, China; 18877571207@163.com (R.L.); jjz19941028@gmail.com (J.J.); lijiahe006@163.com (J.L.); liangxing587@126.com (X.L.)

<sup>2</sup> National Engineering Research Center for Non-Food Biorefinery, State Key Laboratory of Non-Food Biomass and Enzyme Technology, Guangxi Academy of Sciences, Nanning 530004, Guangxi, China

<sup>3</sup> School of Animal Science and Technology, Guangxi University, Nanning 530004, Guangxi, China; yanhao\_day@163.com

<sup>4</sup> Guangxi Key Laboratory of Marine Natural Products and Combinatorial Biosynthesis Chemistry, Guangxi Beibu Gulf Marine Research Center, Guangxi Academy of Sciences, Nanning 530004, Guangxi, China; dengfengyang@163.com

\* Correspondence: panlixia@gxas.cn (L.P.); xietisan@gxu.edu.cn (T.X.); mzmz2009@sohu.com (Z.M.); Tel.: +86-0771-250-3980 (L.P.)

Academic Editors: Simona Collina and Mariarosaria Miloso

Received: 1 July 2020; Accepted: 23 July 2020; Published: date

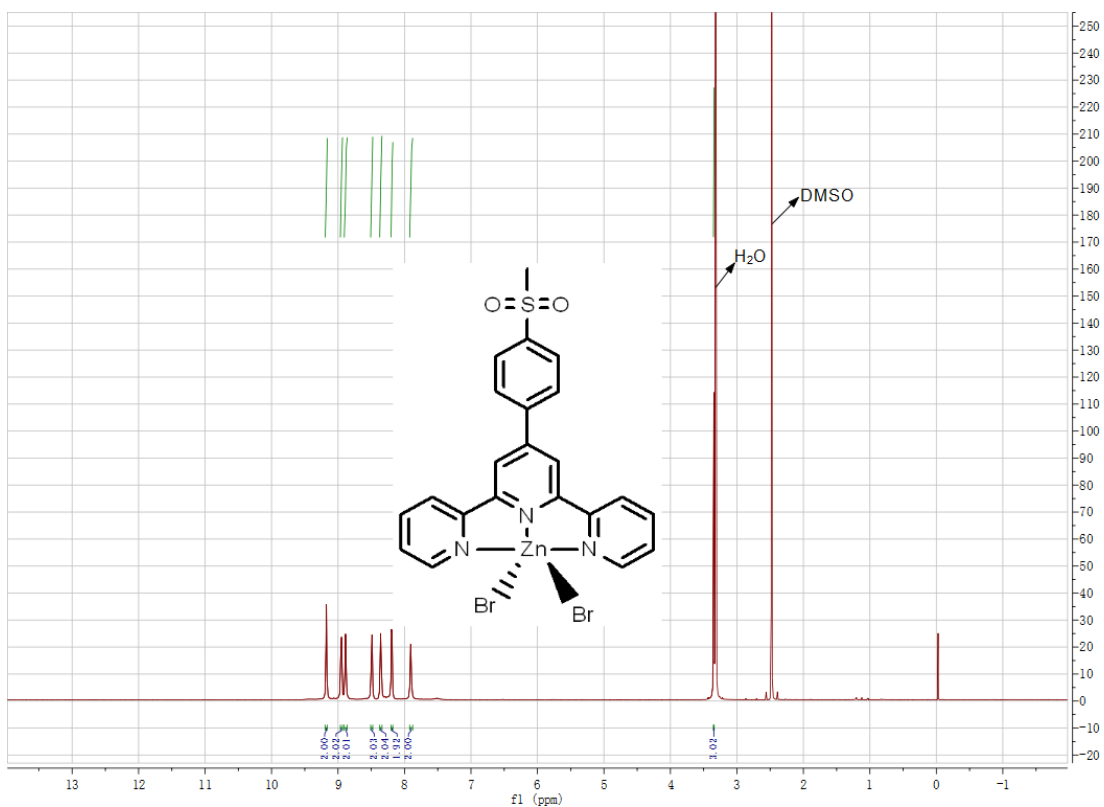


**Figure S1.** The  $^1\text{H}$  NMR spectrum of compound 1.

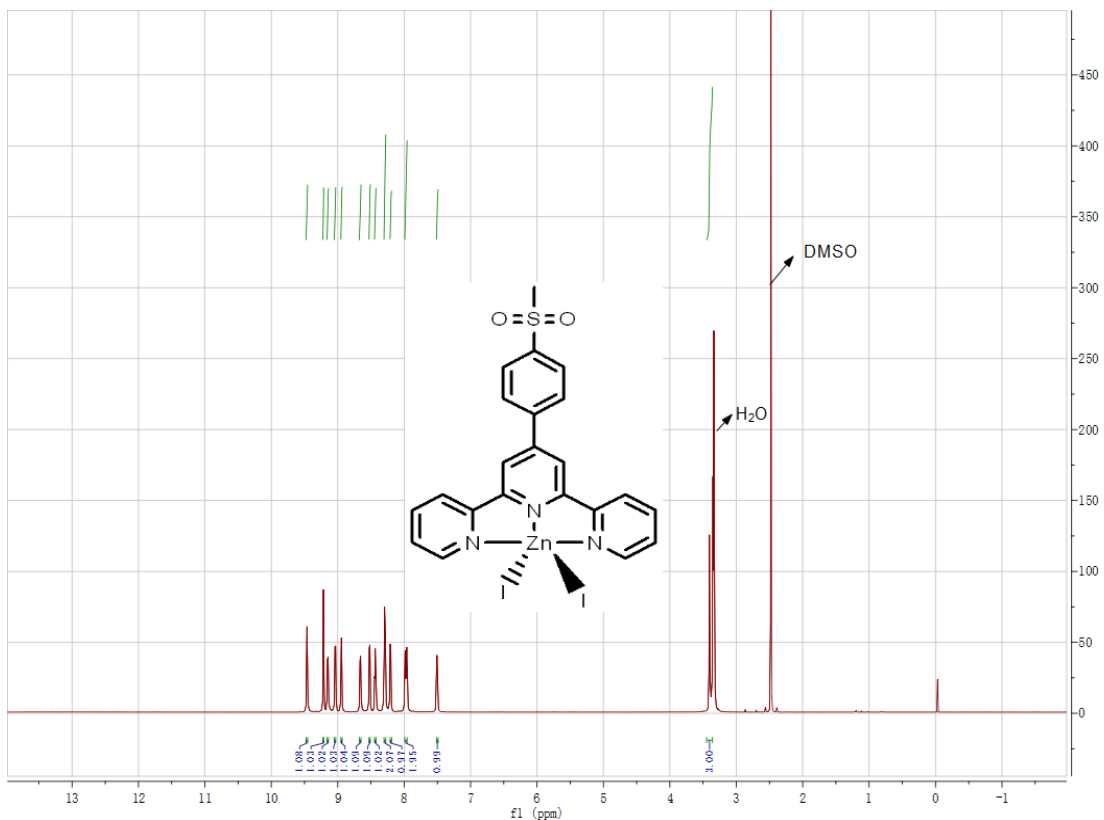


**Figure S2.** The  $^1\text{H}$  NMR spectrum of compound 2.

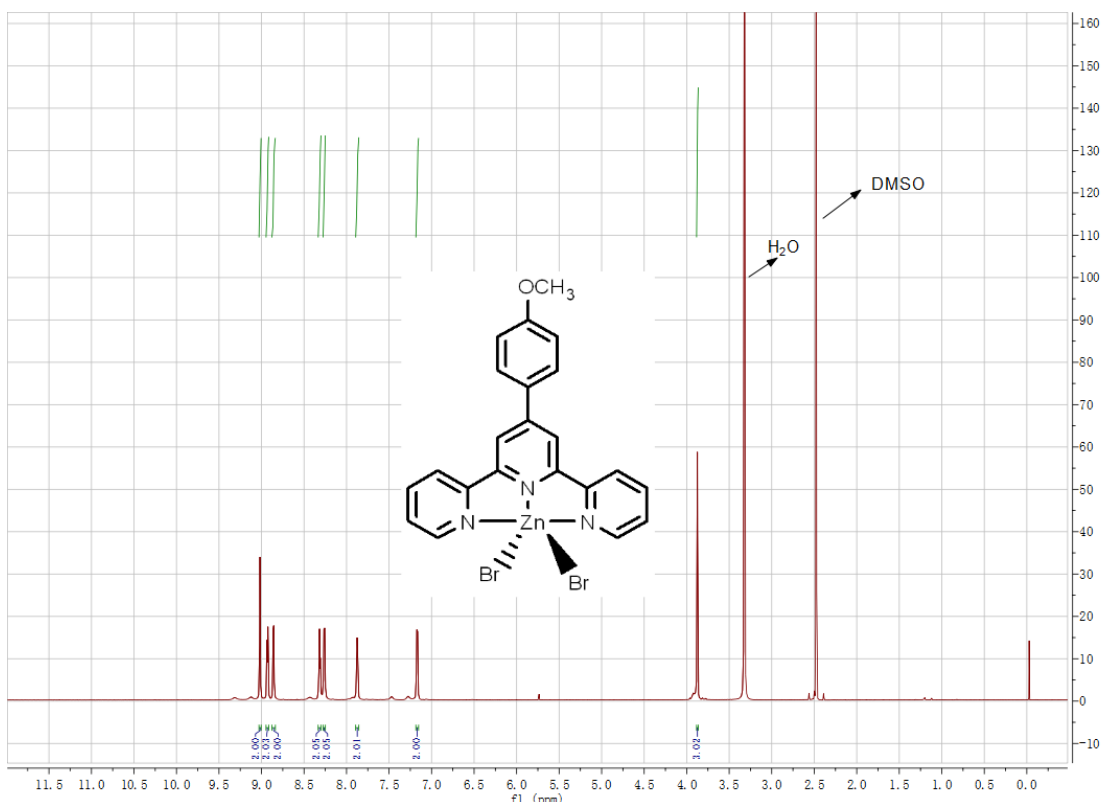


**Figure S3.** The  $^1\text{H}$  NMR spectrum of compound 3.

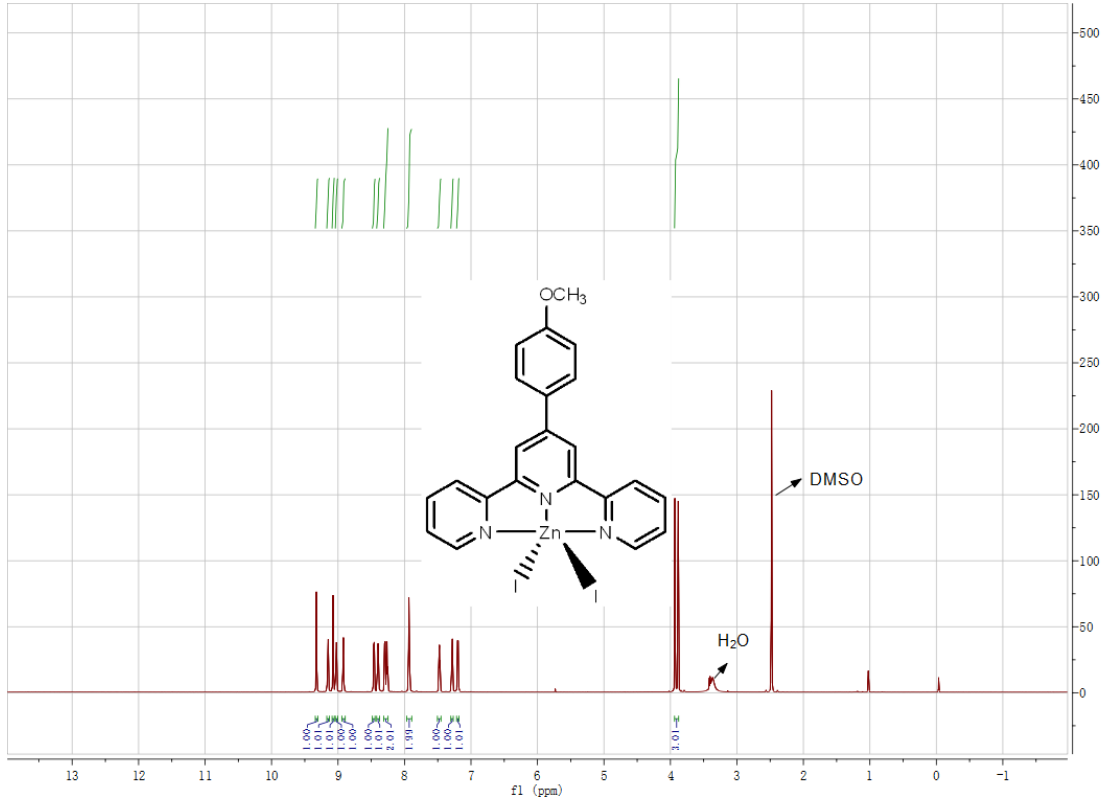


**Figure S4.** The  $^1\text{H}$  NMR spectrum of compound 4.

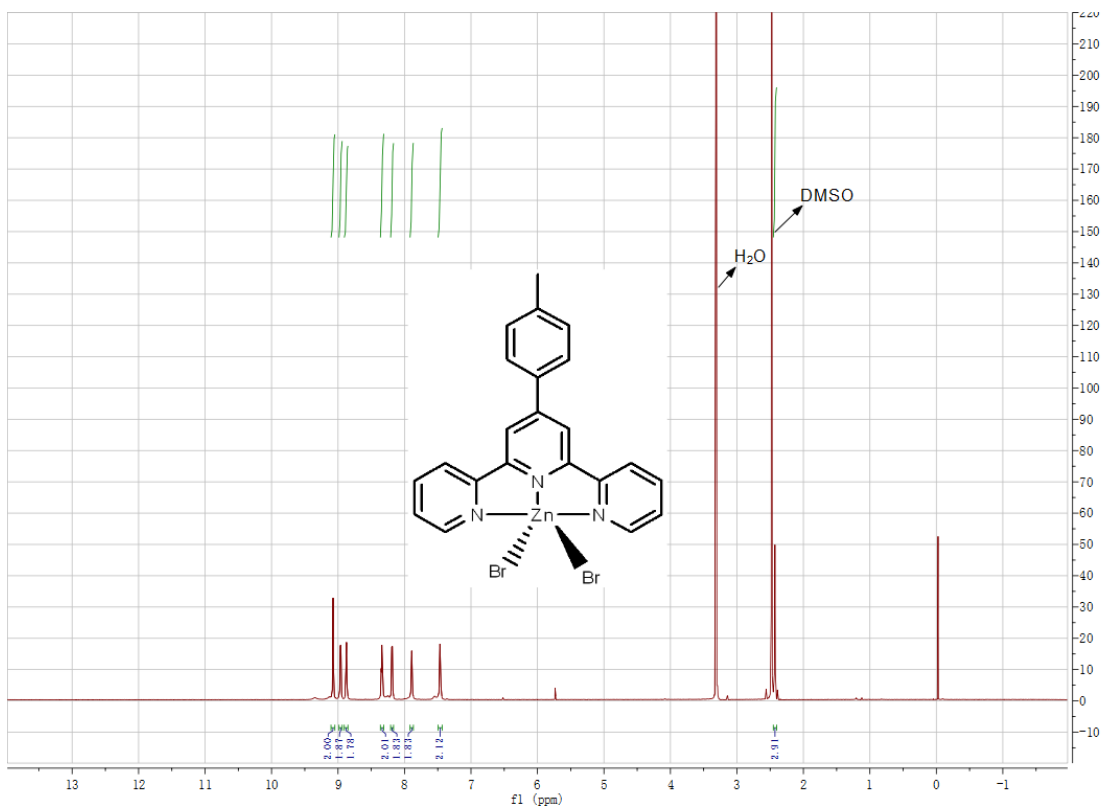


**Figure S5.** The  $^1\text{H}$  NMR spectrum of compound 5.

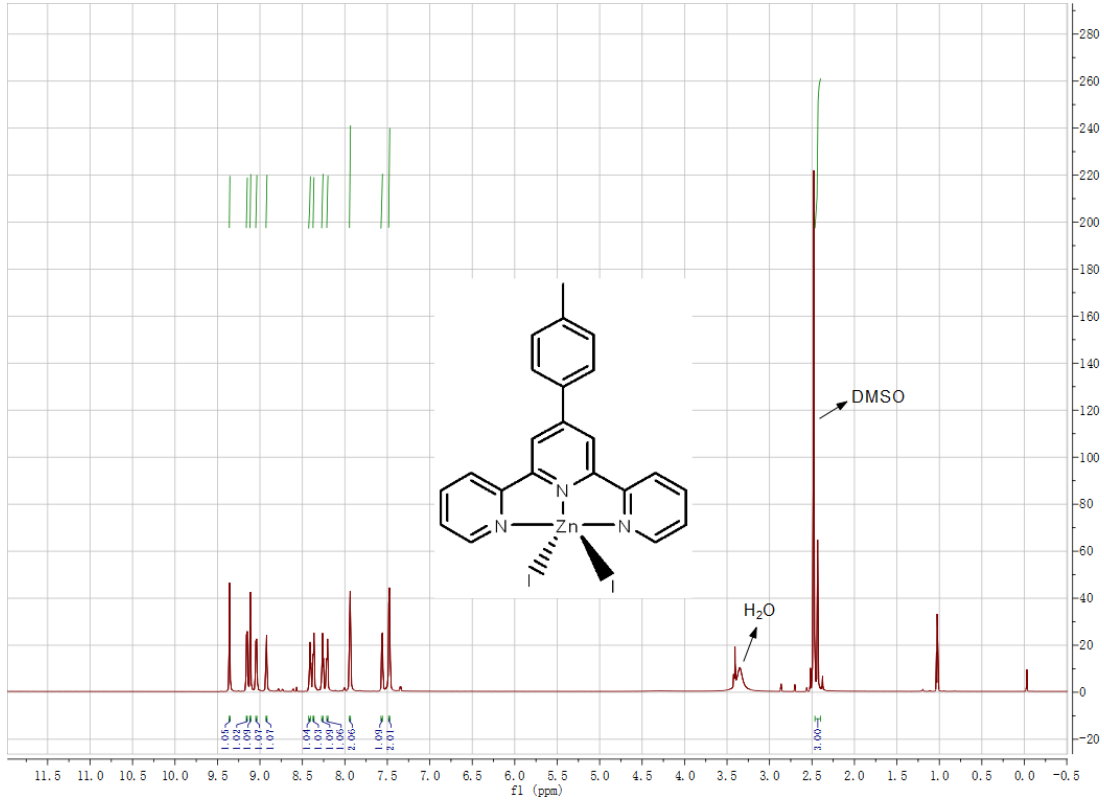


**Figure S6.** The  $^1\text{H}$  NMR spectrum of compound 6.

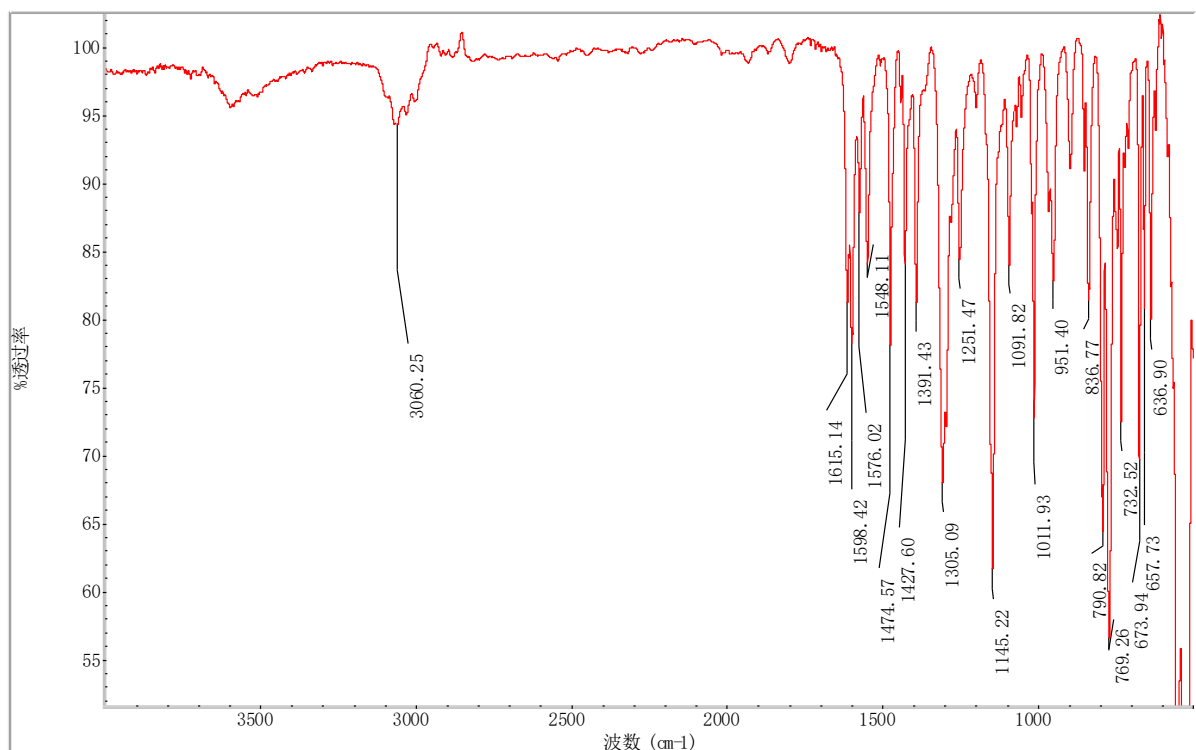


Figure S7. The IR spectrum of compound 1.

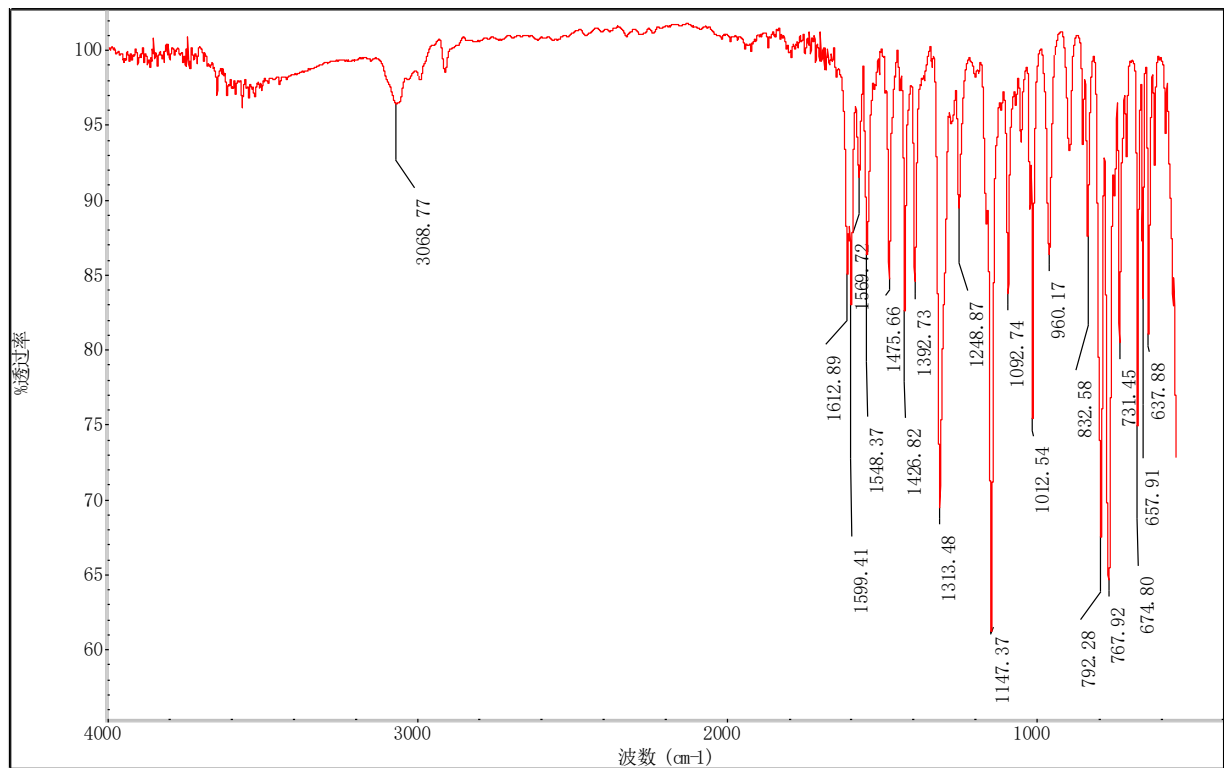


Figure S8. The IR spectrum of compound 2.

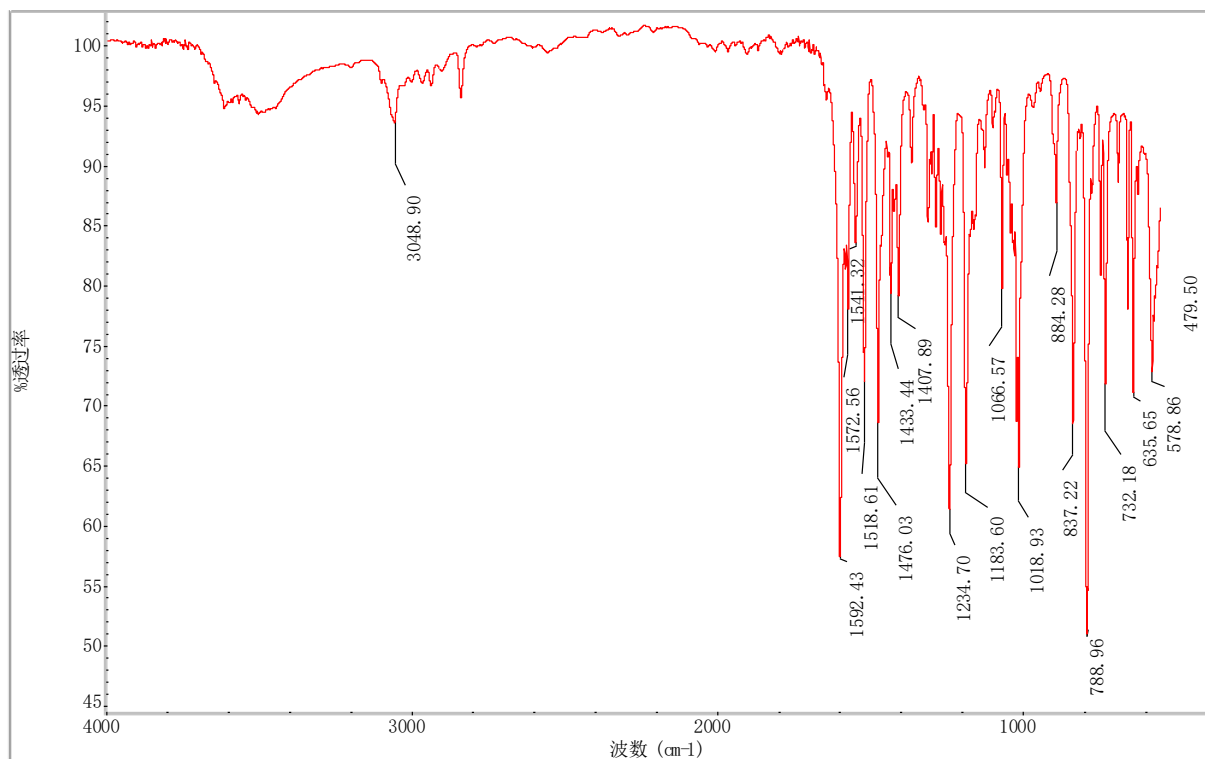


Figure S9. The IR spectrum of compound 3.

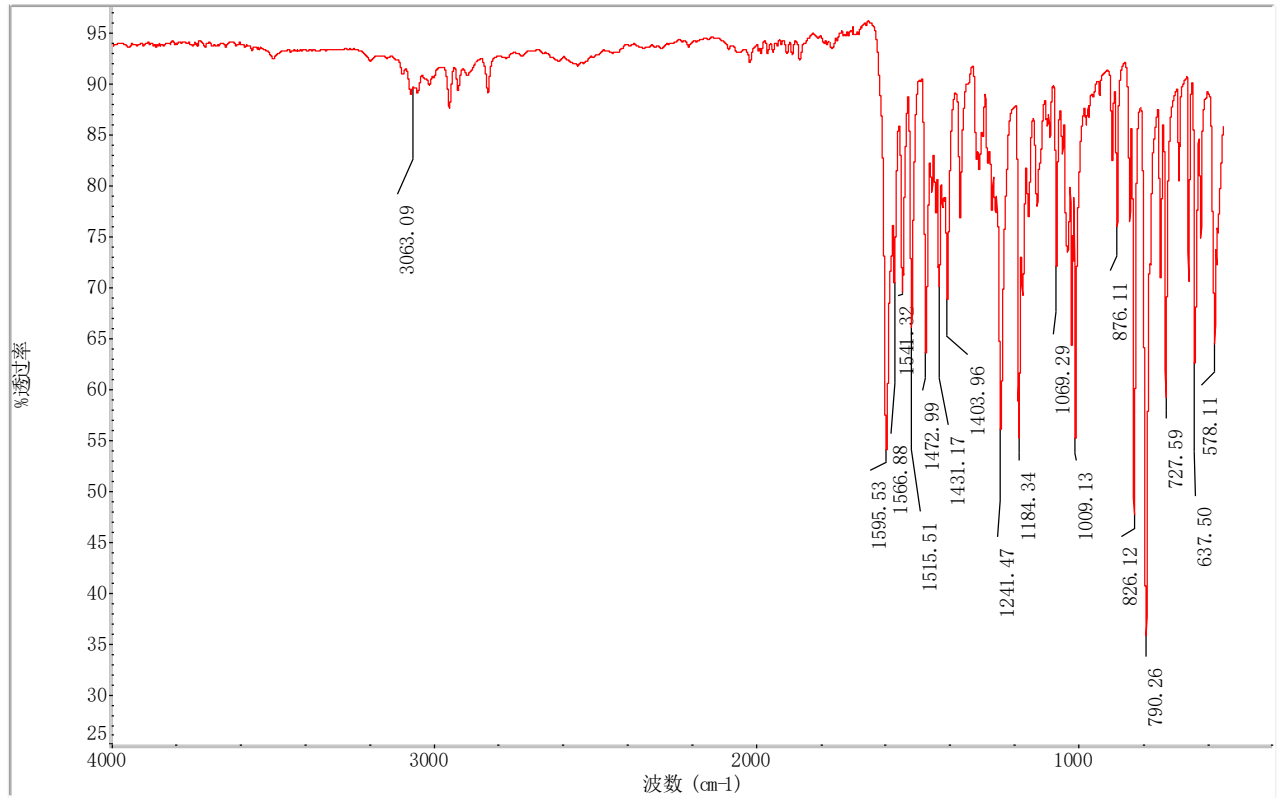


Figure S10. The IR spectrum of compound 4.

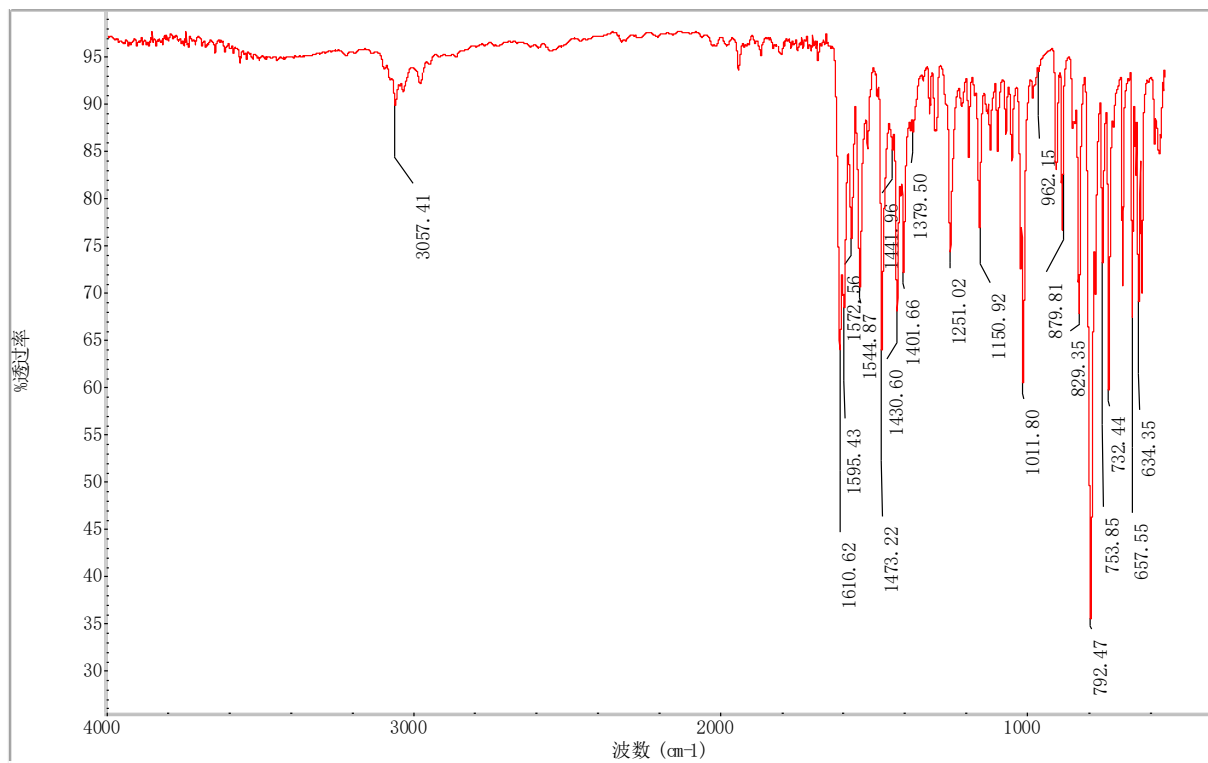


Figure S11. The IR spectrum of compound 5.

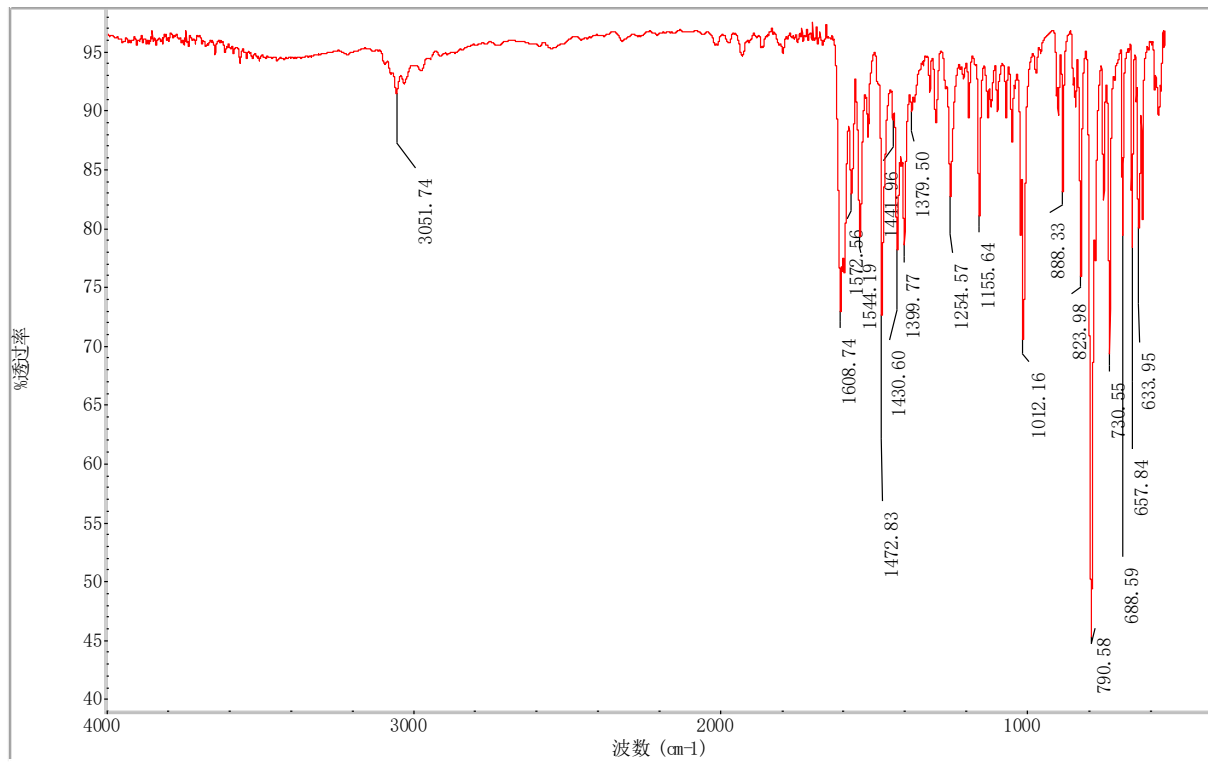
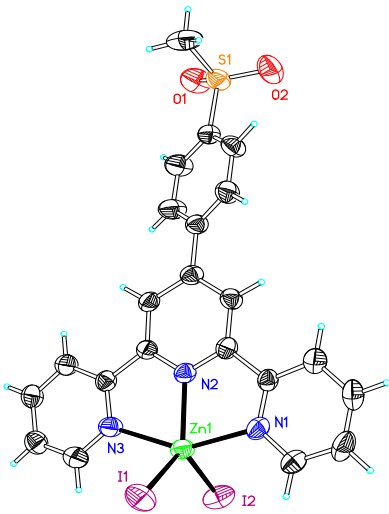
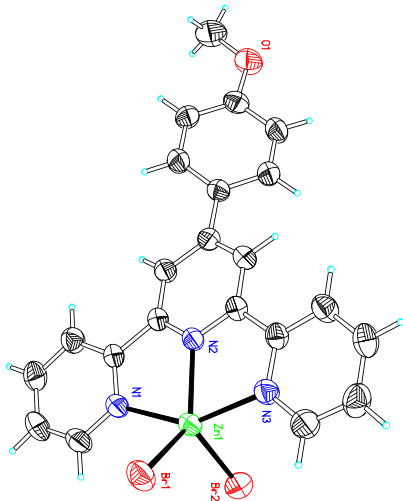


Figure S12. The IR spectrum of compound 6.



**Figure S13.** Thermal ellipsoid plot, drawn at the 50% probability level, of  $[Zn(Br)2L^1]$  (1) with atomic numbering scheme. Selected bond lengths ( $\text{\AA}$ ) and angles ( $^\circ$ ): Zn(1)-N(2) 2.096(3), Zn(1)-N(1) 2.175(4), Zn(1)-N(3) 2.193(3), Zn(1)-I(1) 2.6147(6), Zn(1)-I(2) 2.6170(6); N(2)-Zn(1)-N(1) 74.45(12), N(2)-Zn(1)-N(3) 74.27(12), N(1)-Zn(1)-N(3) 148.71(13), N(2)-Zn(1)-I(1) 121.10(9), N(1)-Zn(1)-I(1) 95.39(10), N(3)-Zn(1)-I(1) 99.93(10), N(2)-Zn(1)-I(2) 118.99(9), N(1)-Zn(1)-I(2) 99.70(10), N(3)-Zn(1)-I(2) 96.06(9), I(1)-Zn(1)-I(2) 119.91(2).



**Figure S14.** Thermal ellipsoid plot, drawn at the 50% probability level, of  $[Zn(Br)2L^1]$  (1) with atomic numbering scheme. Selected bond lengths ( $\text{\AA}$ ) and angles ( $^\circ$ ): Zn(1)-N(2) 2.1086(19), Zn(1)-N(3) 2.209(2), Zn(1)-N(1) 2.228(2), Zn(1)-Br(2) 2.3876(4), Zn(1)-Br(1) 2.4084(4); N(2)-Zn(1)-N(3) 74.45(7), N(2)-Zn(1)-N(1) 73.80(7), N(3)-Zn(1)-N(1) 148.13(8), N(2)-Zn(1)-Br(2) 119.13(6), N(3)-Zn(1)-Br(2) 95.46(6), N(1)-Zn(1)-Br(2) 102.22(6), N(2)-Zn(1)-Br(1) 128.86(6), N(3)-Zn(1)-Br(1) 99.60(6), N(1)-Zn(1)-Br(1) 98.07(6), Br(2)-Zn(1)-Br(1) 111.967(15).

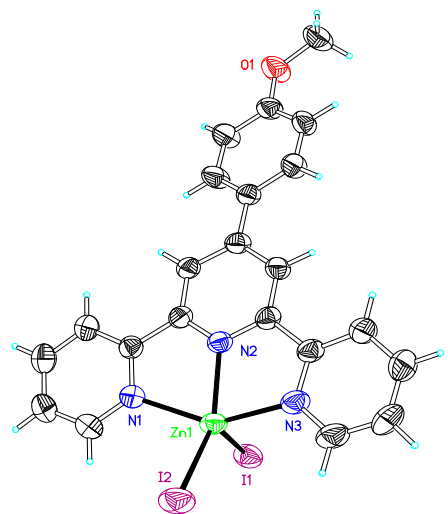


**Figure S15.** Thermal ellipsoid plot, drawn at the 50% probability level, of  $[Zn(Br)2L^1]$  (1) with atomic numbering scheme. Selected bond lengths ( $\text{\AA}$ ) and angles ( $^\circ$ ): Zn(1)-N(2) 2.093(2), Zn(1)-N(1) 2.205(2), Zn(1)-N(3) 2.232(2), Zn(1)-I(2) 2.5919(3), Zn(1)-I(1) 2.6077(4); N(2)-Zn(1)-N(1) 74.64(8), N(2)-Zn(1)-N(3) 73.98(8), N(1)-Zn(1)-N(3) 146.64(8), N(2)-Zn(1)-I(2) 140.76(6), N(1)-Zn(1)-I(2) 97.73(6), N(3)-Zn(1)-I(2) 99.35(6), N(2)-Zn(1)-I(1) 05.09(6), N(1)-Zn(1)-I(1) 97.28(6), N(3)-Zn(1)-I(1) 101.52(7), I(2)-Zn(1)-I(1) 114.104(12).

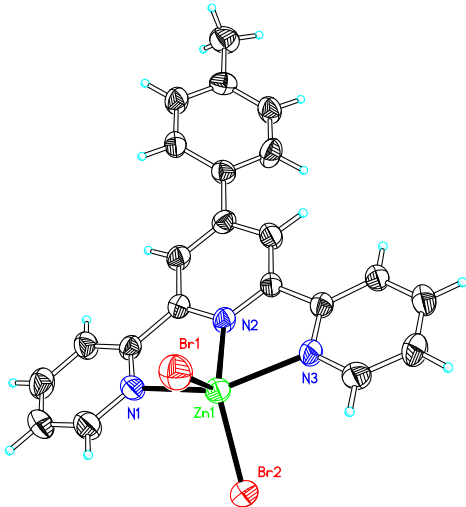


**Figure S16.** Thermal ellipsoid plot, drawn at the 50% probability level, of  $[Zn(Br)2L^1]$  (1) with atomic numbering scheme. Selected bond lengths ( $\text{\AA}$ ) and angles ( $^\circ$ ): Zn(1)-N(2) 2.103(3), Zn(1)-N(1) 2.218(3), Zn(1)-N(3) 2.230(3), Zn(1)-Br(1) 2.3857(7), Zn(1)-Br(2) 2.4062(7); N(2)-Zn(1)-N(1) 74.35(12), N(2)-Zn(1)-N(3) 74.19(11), N(1)-Zn(1)-N(3) 148.49(11), N(2)-Zn(1)-Br(1) 119.44(9), N(1)-Zn(1)-Br(1) 97.02(9), N(3)-Zn(1)-Br(1) 99.89(9), N(2)-Zn(1)-Br(2) 125.84(9), N(1)-Zn(1)-Br(2) 98.36(9), N(3)-Zn(1)-Br(2) 98.43(8), Br(1)-Zn(1)-Br(2) 114.70(2).

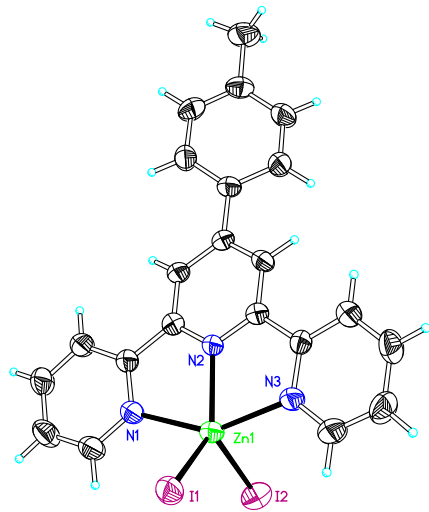


**Figure S17.** Thermal ellipsoid plot, drawn at the 50% probability level, of  $[Zn(Br)_2L^1]$  (1) with atomic numbering scheme. Selected bond lengths ( $\text{\AA}$ ) and angles ( $^\circ$ ): Zn(1)-N(2) 2.095(3), Zn(1)-N(3) 2.221(3), Zn(1)-N(1) 2.232(3), Zn(1)-I(2) 2.5838(5), Zn(1)-I(1) 2.6051(5); N(2)-Zn(1)-N(3) 74.36(11), N(2)-Zn(1)-N(1) 73.94(11), N(3)-Zn(1)-N(1) 147.98(12), N(2)-Zn(1)-I(2) 118.23(8), N(3)-Zn(1)-I(2) 97.98(9), N(1)-Zn(1)-I(2) 100.82(9), N(2)-Zn(1)-I(1) 129.08(8), N(3)-Zn(1)-I(1) 97.59(8), N(1)-Zn(1)-I(1) 98.76(8), I(2)-Zn(1)-I(1) 112.661(18).

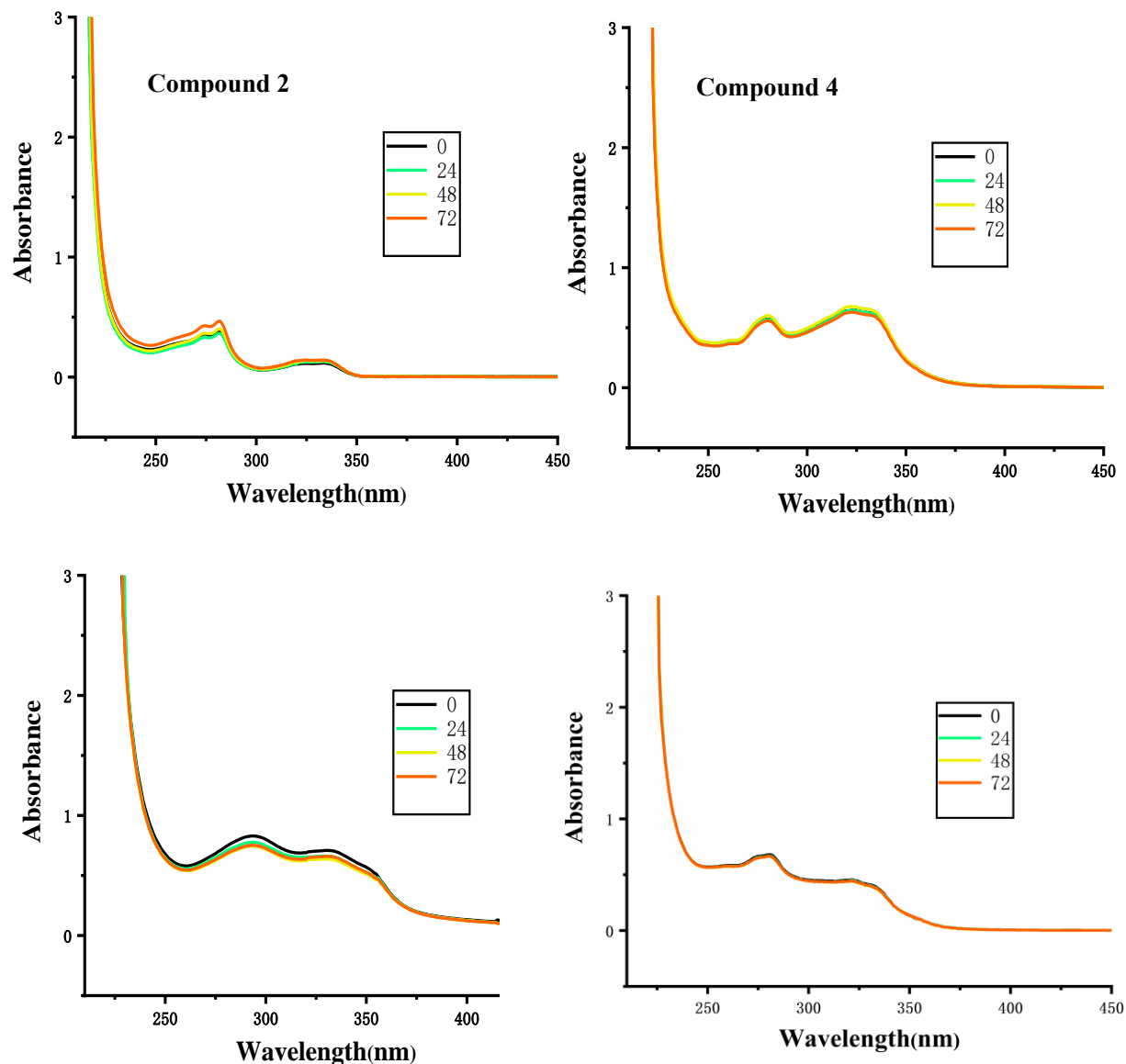


**Figure S18.** The UV-vis spectra of complexes **2**, **4**, **5** and **6** in PBS buffer solution over a period of 72h.

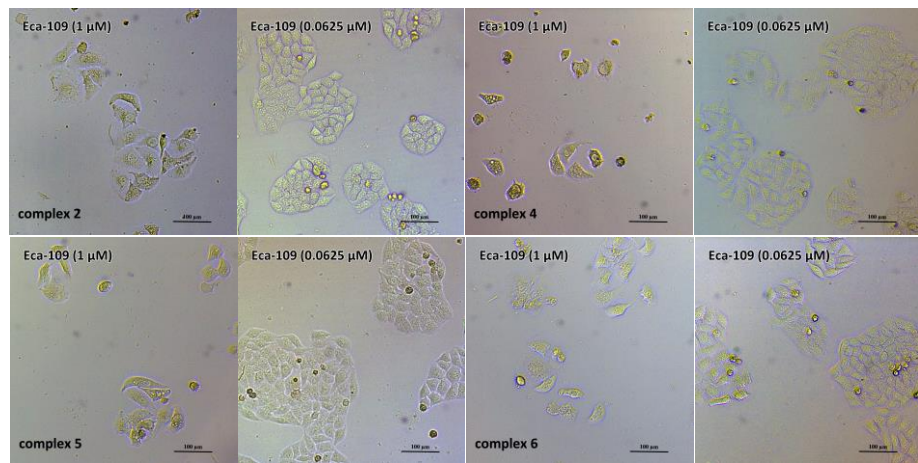


**Figure S19.** The microscopic photographs of Eca-109 cancer cells treated with different concentrations of compound **2, 4, 5 and 6**.

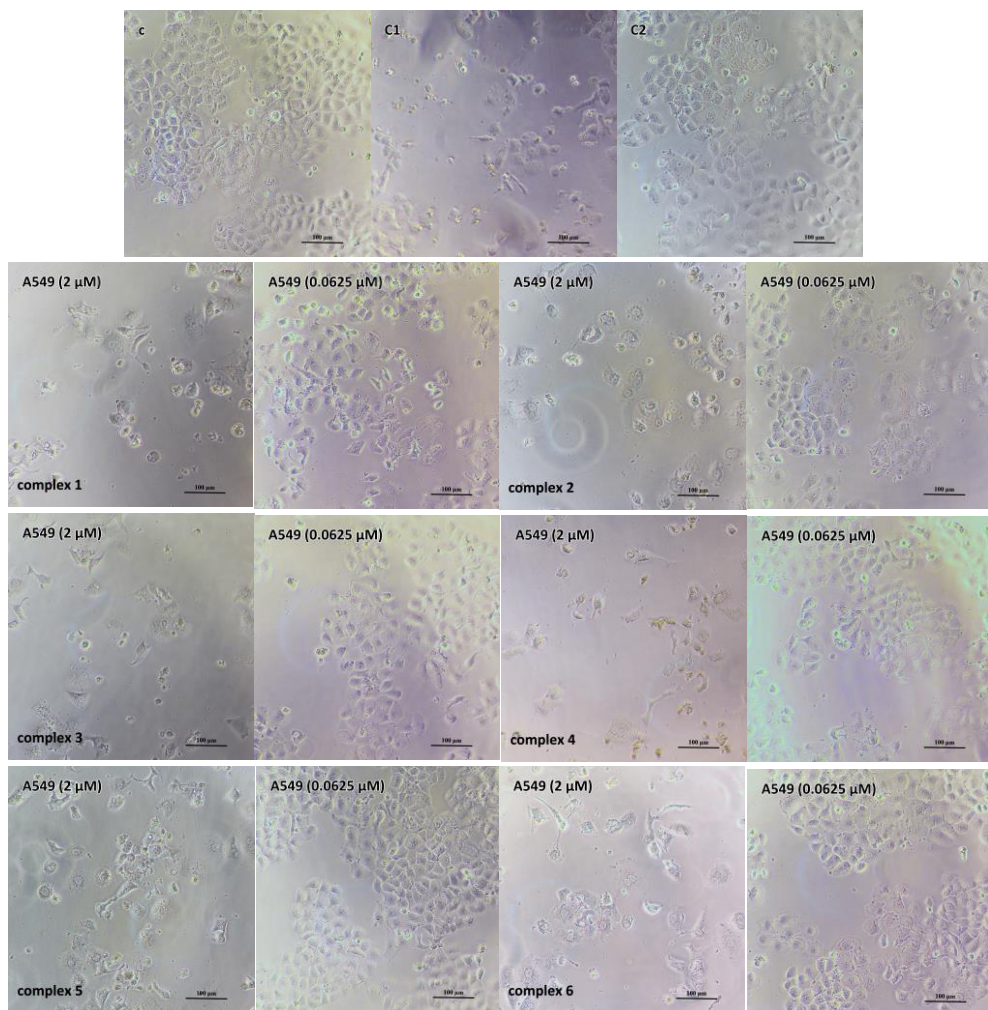


**Figure S20.** The microscopic photographs of A549 cancer cells treated with different concentrations of compounds and control photographs (C for blank group, C1 for 5  $\mu$ M cisplatin and C2 for 40  $\mu$ M cisplatin).

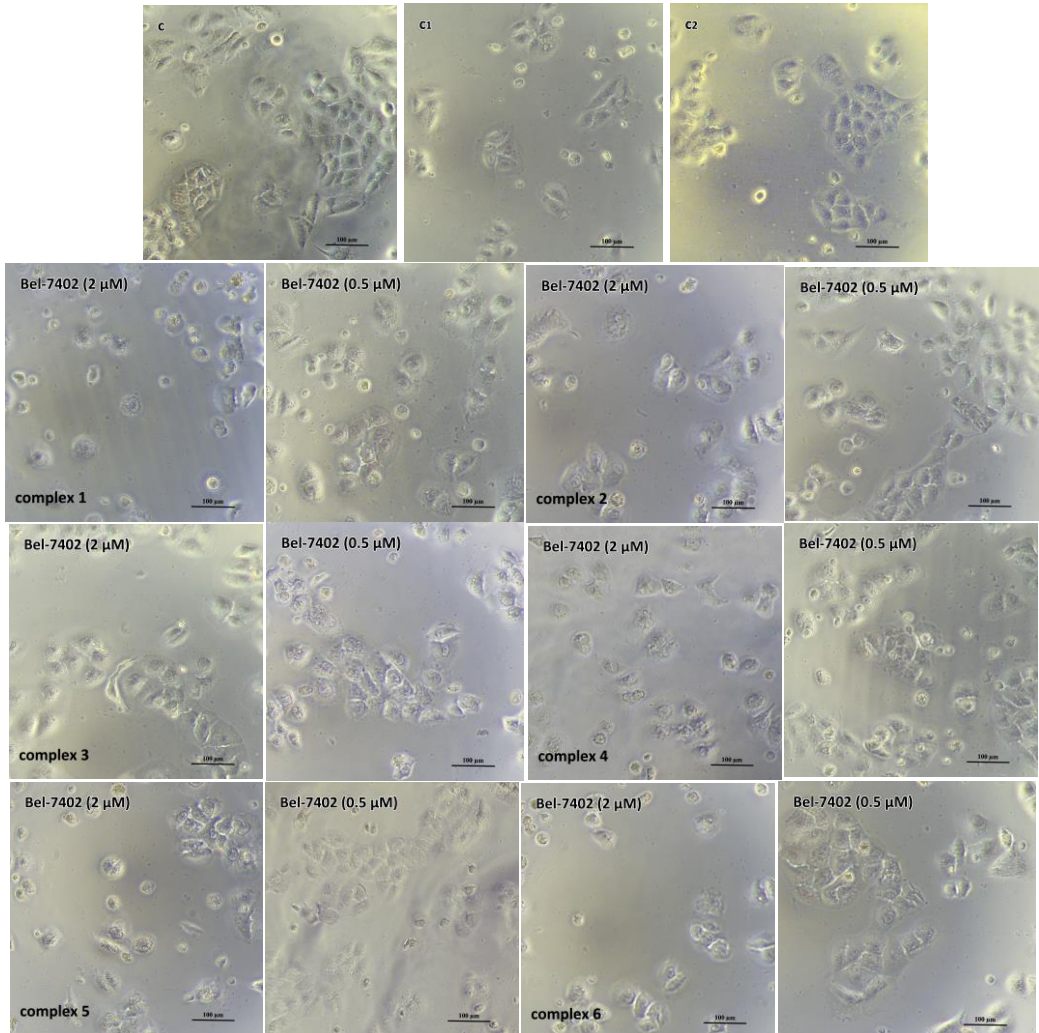


**Figure S21.** The microscopic photographs of Bel-7402 cancer cells treated with different concentrations of compounds and control photographs (**C** for blank group, **C1** for 2.5  $\mu$ M cisplatin and **C2** for 5  $\mu$ M cisplatin).

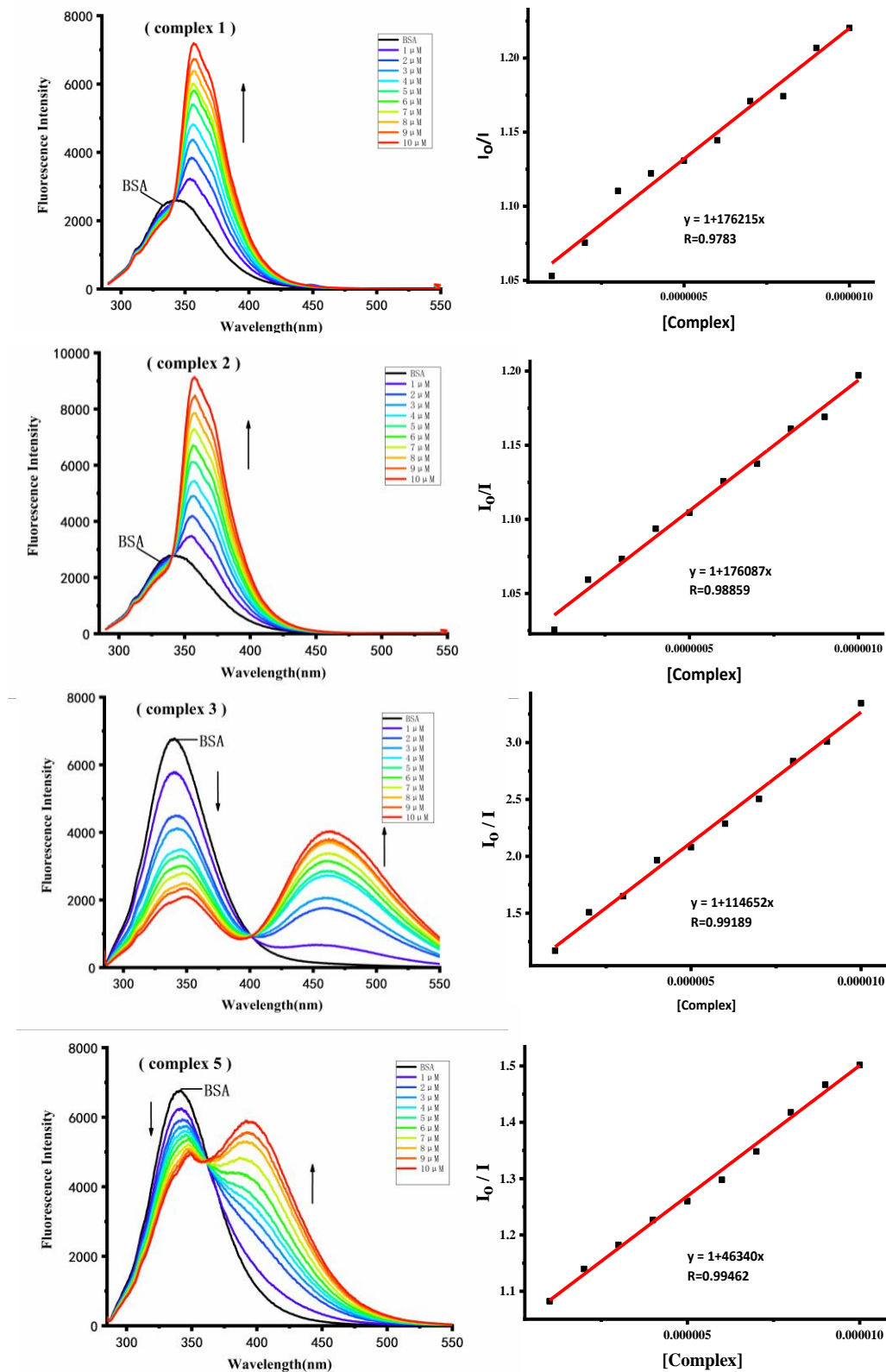


**Figure S22.** Fluorescence emission spectra of 1.6 μM BSA in Tris-HCl buffer (PH = 7.2) solution with series concentration of compound **1**, **2**, **3** and **5**, and the curves for Stern-Volmer equation as the insets.

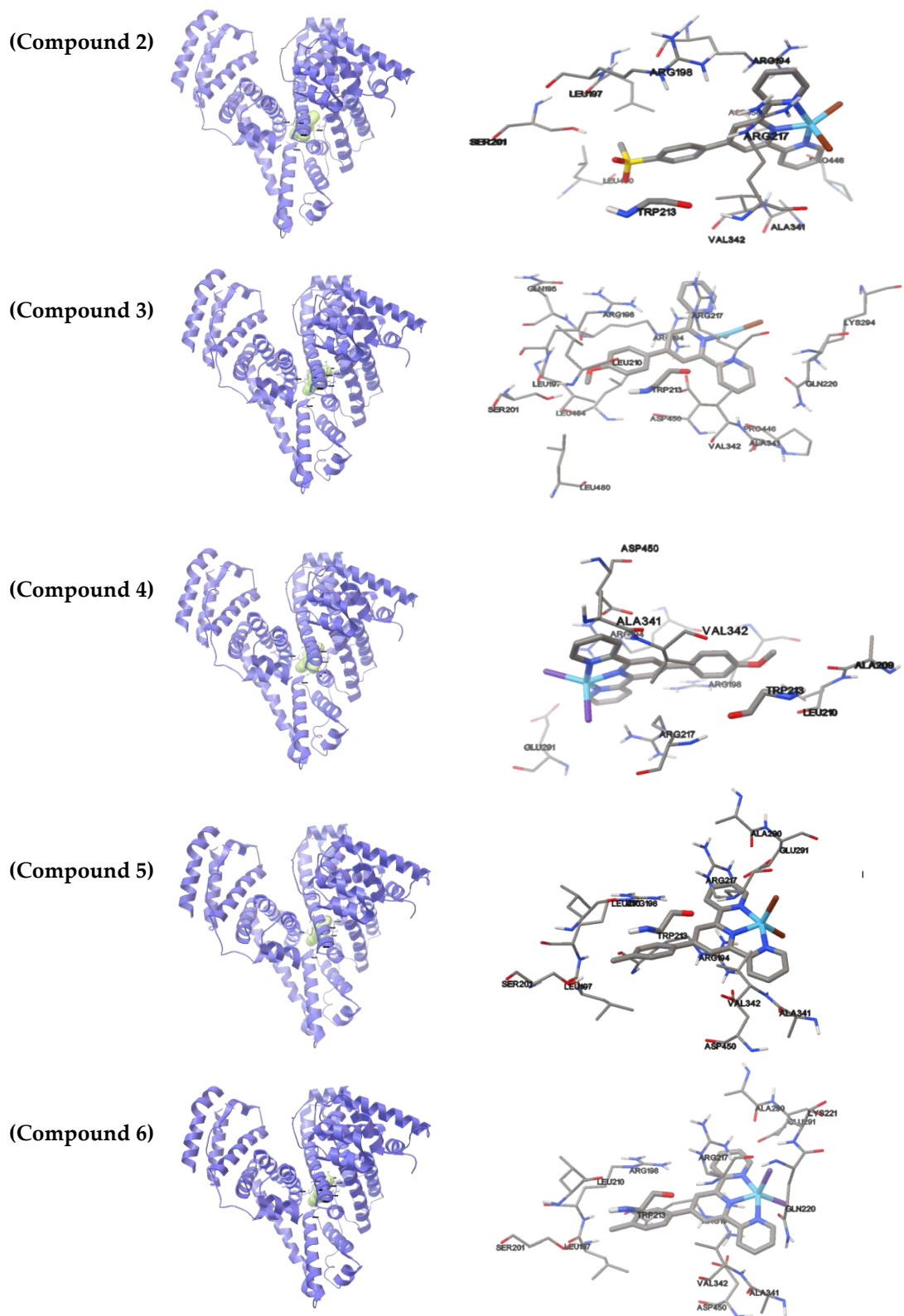


**Figure S23.** The docking conformation of complexes 2–6 to BSA, and amino acid residues surrounding compounds 2–6.

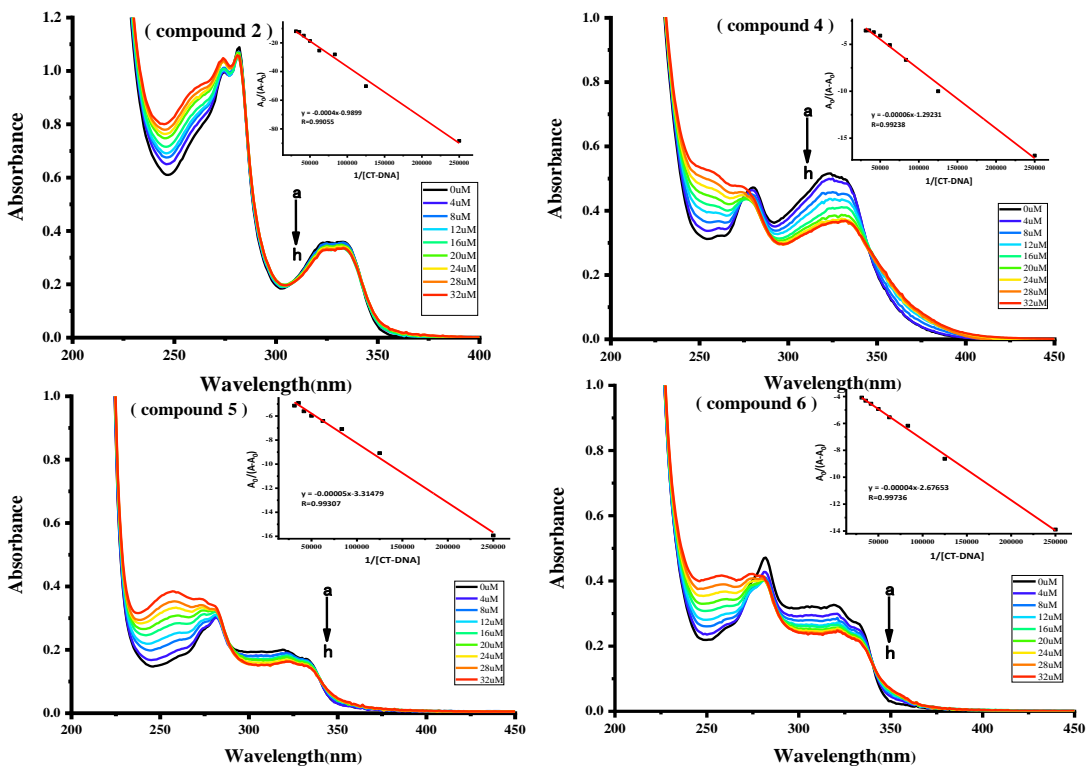


**Figure S24.** Absorption spectra of 20 $\mu$ M compounds 2, 4, 5 and 6 in Tris-HCl buffer (PH=7.2) solution with series concentration of CT-DNA, The plots of  $A_0/(A - A_0)$  versus the concentration of CT-DNA as the insets.

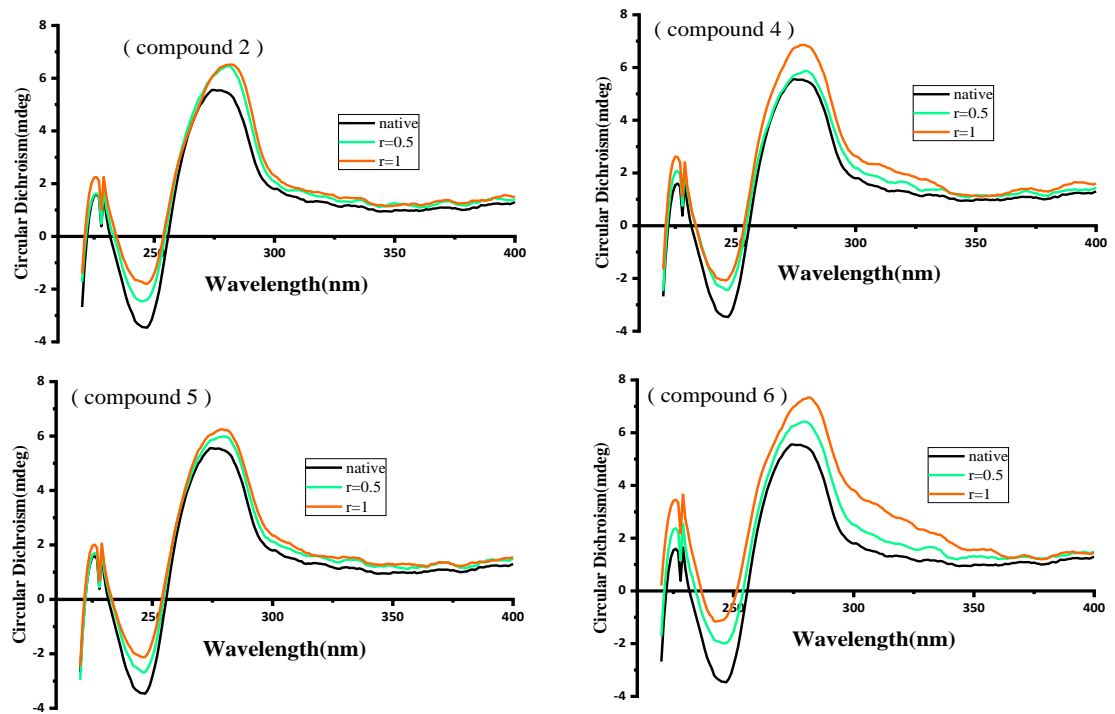


**Figure S25.** CD spectra of compounds 2, 4, 5 and 6 to CT-DNA at different concentration ratios.

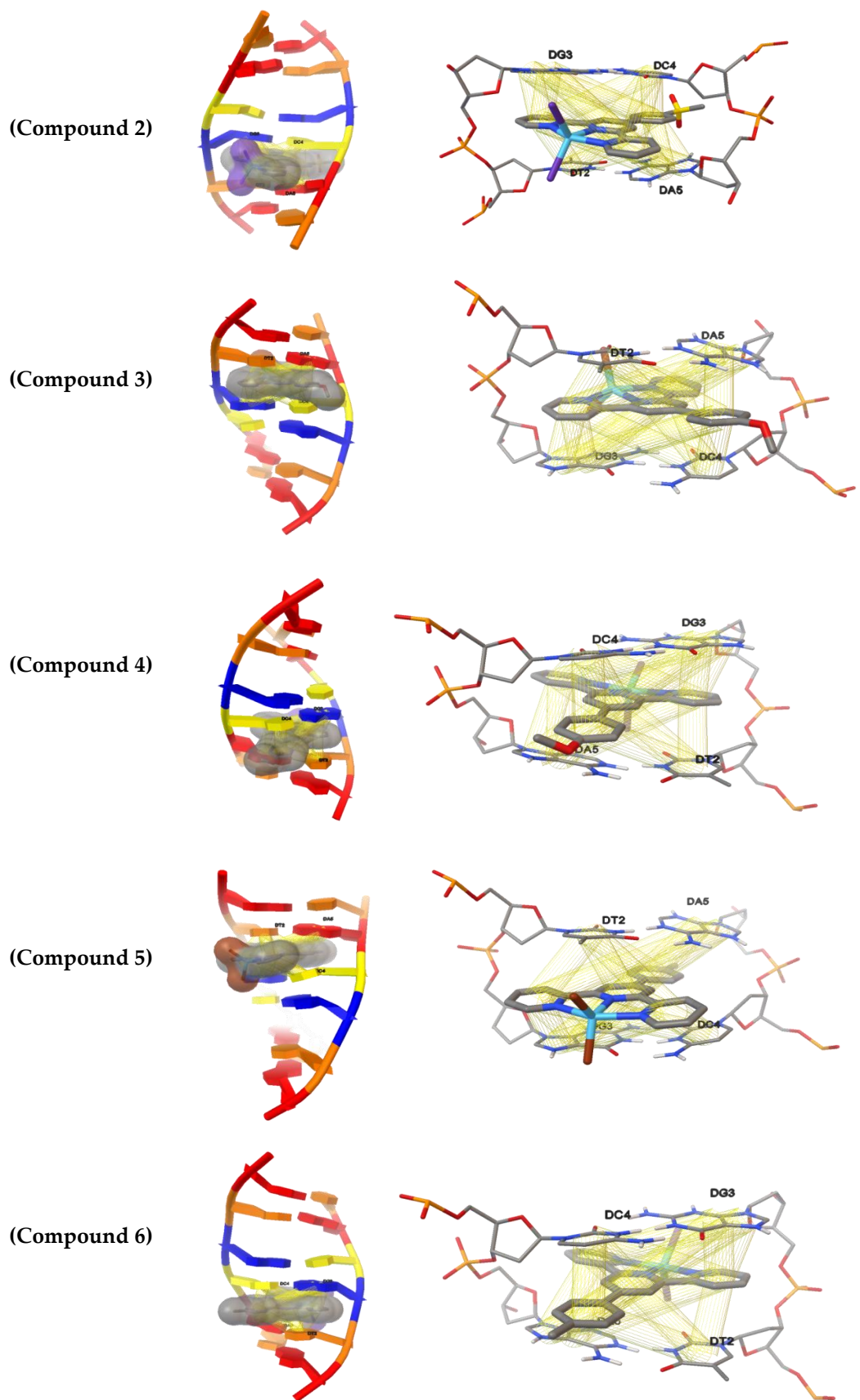


**Figure S26.** The docking conformation of complexes 2–6 to DNA (PDB ID: 4JD8).